Biochemical Pharmacology 78 (2009) 941–950

Contents lists available at ScienceDirect

Biochemical Pharmacology

journal homepage: www.elsevier.com/locate/biochempharm

A novel marine compound xyloketal B protects against oxidized LDL-induced cell injury in vitro

Wen-Liang Chen [a], Yan Qian [a], Wei-Feng Meng [a], Ji-Yan Pang [b,c], Yong-Cheng Lin [b,c], Yong-Yuan Guan [a], Sheng-Pin Chen [c], Jie Liu [a], Zhong Pei [d,**], Guan-Lei Wang [a,c,*]

[a] Department of Pharmacology, Zhongshan School of Medicine, Sun Yat-Sen University, 74 Zhongshan Road II, Guangzhou, 510080, PR China
[b] Department of Applied Chemistry and Department of Pharmacy, Sun Yat-Sen University, Guangzhou, 510080, PR China
[c] Key Laboratory of Functional Molecules from Oceanic Microorganisms (Sun Yat-sen University), Department of Education of Guangdong Province, 510080, PR China
[d] Department of Neurology, The First Affiliated Hospital, Sun Yat-Sen University, 58 Zhongshan Road II, Guangzhou, 510080, PR China

ARTICLE INFO

Article history:
Received 5 April 2009
Accepted 20 May 2009

Keywords:
Xyloktals
Endothelial cells
Oxidized low-density lipoprotein
Reactive oxygen species
Nitric oxide
Nicotinamide adenine dinucleotide phosphate oxidase

ABSTRACT

Xyloketal B is a novel marine compound with unique chemical structure isolated from mangrove fungus *Xylaria* sp. (no. 2508). Pretreatment with xyloketal B (0.63–40 μM) significantly improved oxLDL (150 μg/ml)-induced injury in human umbilical vein endothelial cells (HUVECs) without either toxic or proliferative effects. Xyloketal B concentration-dependently attenuated oxLDL-induced ROS generation, peroxynitrite formation and decrease of Bcl-2 expression. In addition, xyloketal B significantly inhibited NADPH oxidase activity, as well as mRNA expression of gp91*phox* and p47*phox*. Furthermore, xyloketal B alone augmented the production of nitric oxide (NO). Collectively, these data indicate that xyloketal B protects against oxLDL-induced endothelial oxidative injury probably through inhibiting NADPH oxidase-derived ROS generation, promoting NO production and restoring Bcl-2 expression, making it a promising compound for further evaluation in the treatment of atherosclerosis.

1. Introduction

Vascular endothelial cell injury elicited by oxidatively modified low-density lipoprotein (oxLDL) is critically important in the pathogenesis of atherosclerosis. OxLDL-induced endothelial cell apoptosis is associated with not only initiation of plaque development, but also plaque destabilization and thrombosis in atherosclerosis [1].

The disturbed balance between reactive oxygen species (ROS) and nitric oxide (NO) is the major cause of oxLDL-induced endothelial cell apoptosis [1]. When oxLDL binds to scavenger receptors [e.g., LOX-1(lectin-like ox-LDL receptor-1)], it rapidly stimulates excessive ROS generation including superoxide anions and hydrogen peroxide via activation of NADPH oxidase, reducing local nitric oxide (NO) production and antioxidant capability in body [2,3], at the same time, reduced NO generation or reduced NO bioavailability also largely contributes to endothelial dysfunction. Physiologically, endothelial derived NO can inhibit platelet aggregation and have an anti-atherosclerotic effect. [4]. However, NO is reduced by excess ROS generated under oxidative stress condition. Furthermore, excess ROS can react with NO to produce peroxynitrite, a very potent oxidant. Peroxynitrite in turn oxidize protein and cause further tissue damage and loss of function [5–7].

Marine organisms are an excellent natural source of novel bioactive compounds because they can produce a variety of molecules with unique structural features and exhibit various types of biological activities [8]. Xyloketal B, is one of a series of novel ketal compounds isolated from mangrove fungus *Xylaria* sp. (no. 2508), obtained from the South China Sea (Fig. 1) [9,10]. Recently, we found that xyloketal B can relax the phenylephrine-induced contraction of rat thoracic aorta rings, attenuate the increasing blood pressure and myocardial remodeling in two-kidney, two-clip stroke-prone hypertensive rat model (unpublished data). The hydroxy-phenol radical in xyloketal B indicates that it may have antioxidant and free radical scavenging properties. In the present study, we investigated whether xyloketal B can protect against oxLDL-induced human umbilical vein endothelial

Abbreviations: OxLDL, oxidatively modified low-density lipoprotein; Xyl-B, xyloketal B; ROS, reactive oxygen species; NO, nitric oxide; $ONOO^-$, peroxynitrite; EC, endothelial cell; DCFH-DA, 2′,7′-dichlorofluorescin diacetate; DAF-FM DA, 3-amino,4-aminomethyl-2′,7′-difluorescein, diacetate; HUVECs, human umbilical vein endothelial cells; eNOS, endothelial nitric-oxide synthase; L-NAME, N(G)-nitro-L-arginine methyl ester; 3-NT, 3-nitrotyrosine; DAPI, 4′,6-diamidino-2-phenylindole; Apo, apocynin.

* Corresponding author at: Department of Pharmacology, Zhongshan School of Medicine, Sun Yat-Sen University, 74 Zhongshan Road II, Guangzhou, 510080, PR China. Tel.: +86 20 87331155; fax: +86 20 87331155.
** Corresponding author. Tel.: +86 20 87755766/8282.
E-mail addresses: peizhong@mail.sysu.edu.cn (Z. Pei), wanggleI@mail.sysu.edu.cn (G.-L. Wang).

0006-2952/$ – see front matter © 2009 Elsevier Inc. All rights reserved.
doi:10.1016/j.bcp.2009.05.029

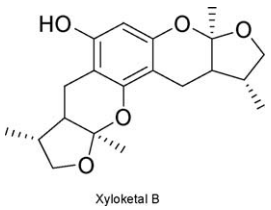

Fig. 1. The structure of xyloketal B.

cell (HUVEC) injury and explore its potential actions on oxidative signaling events including ROS generation, peroxynitrate generation, NO production, and the activity of NADPH oxidase and the mRNA expression of NADPH oxidase components.

2. Materials and methods

2.1. Reagents

Medium 199, fetal calf serum was purchased from Gibco, USA. All other reagents utilized were purchased from Sigma Chemical Co. USA unless otherwise specified. Xyloketal B was isolated by Department of Applied Chemistry and Department of Pharmacy, Sun Yat-Sen University, China. The identity and purity of the compound was determined using HPLC (high performance liquid chromatography) and 2D NMR as previously described [9] and were >99%. Xyloketal B was dissolved in dimethyl sufoxide (DMSO) and stored at −20 °C until use. Final concentration of DMSO in culture media was ≤0.1%.

2.2. Cell culture

Human umbilical vein endothelial cells were isolated and cultured as previously described [11]. Briefly, HUVECs were removed from human umbilical veins after collagenase type I digestion, and cultured in medium 199 containing 20% fetal calf serum, penicillin (100 U/ml), streptomycin (100 U/ml), and heparin (50 U/ml), supplemented with L-glutamine (2 mM), sodium pyruvate (1 mM), and endothelial cell growth factor (β-ECGF, 5 ng/ml), at 37 °C in 5% CO_2 on 0.1% gelatin-coated culture flasks. Endothelial cells were identified by their morphology which appears "cobblestone" mosaic appearance after reaching confluence and the presence of von Willebrand factor. Passage 3–6 HUVECs were used for experiments.

2.3. Preparation of native LDL and oxLDL

Native LDL (d = 1.019–1.063) was isolated from fresh human plasma by sequential ultracentrifugation as previously described [12]. Venous blood from healthy adult donors was obtained from the Guangzhou Blood Center. Blood was collected in tubes containing 1 mg/ml EDTA and immediately centrifuged at 1750 g at 4 °C. Plasma was adjusted to a density of 1.20 g/ml by adding solid NaBr, with gentle stirring, after the previous addition of EDTA (1 mM final concentration). The plasma solution was then distributed into 8-ml polycarbonate centrifuge tubes and a discontinuous density gradient was made by overlaying the plasma solution (3.0 ml) with 2.5 ml phosphate-buffered saline (d = 1.019 g/ml) and 2.5 ml phosphate-buffered saline (d = 1.063 g/ml) containing 1 mM EDTA, saturated with nitrogen. The tubes were ultracentrifuged at 60,000 rpm for 5 h at 4 °C with slow acceleration and deceleration (OPTIMA MLA-80 K; Beckmann, Fullerton, CA, USA). After centrifugation, the tubes were carefully removed from the rotor and placed in the vertical position. The yellow-orange LDL fraction stays in the upper half of the tube. The LDL fraction was collected by suction using a 2 ml injector. Native LDL was oxidized by adding Copper sulphate (5 μM) for 24 h [13]. In our experiments, the thiobarbituric acid-reactive substance content of oxLDL was 12.5 ± 0.68 vs. 0.67 ± 0.26 nM/100 μg protein in the native LDL preparation ($P < 0.01$). The distance of oxLDL migration was compared to that of native LDL and expressed as relative electrophoretic mobility (2.1 ± 0.3, arbitrary units). The concentrations of native LDL and oxLDL were measured using BCA kit (Beyotime, China) and expressed as micrograms per milliliter of solution. Lipoproteins were stored at 4 °C in the dark and freshly prepared every 2 weeks.

2.4. Cell viability assay

Cell viability was assessed by the mitochondrial tetrazolium assay (MTT) in HUVECs. Confluent cells were treated with various concentration of xyloketal B or vehicle for 48 h. MTT solution (10 μl/well) was added and processed to examine cell viability. Optical density was read at 570 nm by Biotek Elx-800 plate reader. Cells alone were used as control group and the cell viability of control group was taken as 100%. At tested concentrations, xyloketal B showed no significant effects on cell viability in both cell types. To exclude possible toxicity from solvent, various concentrations of DMSO were incubated with each cell types, respectively, No toxicity was detected at the concentrations used in the present study.

To test the effects of xyloketal B on oxLDL-induced cell injury in HUVECs, HUVECs were incubated with LDL or oxLDL for 24 h. Xyloketal B was added 0.5 h prior to oxLDL.

2.5. Observation of morphological changes

2.5.1. Inverted microscopy study

In 60 mm culture dishes, HUVECs were preincubated with xyloketal B or vehicle for 30 min, and exposed to oxLDL (150 μg/ml) for further 24 h. The morphological changes were then observed under an inverted microscope (Nikon TS100, Japan). Images were captured randomly using Olympus digital camera (Olympus, Japan). Five non-overlapping fields of view were randomly captured per dish.

2.5.2. DAPI staining

HUVECs were fixed in 4% paraformaldehyde for 15 min, and then incubated with 2.5 μg/ml of DAPI (Molecular Probes, USA) for 30 min at room temperature. Photographed Nuclei were visualized using laser confocal microscope. Cells with condensed chromatin or shrunken, irregular, or fragmented nuclei were considered apoptotic. Apoptotic values were calculated as the percentage of apoptotic cells relative to the total number of cells in each random field (>200 cells).

2.6. ROS measurement

Reactive oxygen species (ROS) in HUVECs was visualized by 2′,7′-dichlorofluorescin diacetate (DCFH-DA, SIGMA, USA) as previously described [3,14]. To optimize the stimulated concentration of oxLDL and incubation time, confluent HUVECs in 35 mm Petri dishes or 96-well clear bottom black microtiter plates (Corning Incorporated) were treated with different concentrations of oxLDL for 30, 60 and 90 min, respectively. And as shown in results, the concentration of 150 μg/ml and incubation time of 90 min was fixed in the following experiments for oxLDL stimulation. To examine the effects of xyloketal B, After loading cells with DCFH-DA (10 μM) in serum free M199 for 60 min at 37 °C, cells were pretreated for 30 min with 0.2–40 μM xyloketal B, respectively, followed by native LDL or oxLDL (150 μg/ml) incubation for 90 min. The fluorescence intensity in Petri dishes

was measured at 485-nm excitation and 538-nm emission using a laser confocal scanning microscopy (FV500, Olympus, Japan). Fluoview 500 software was used to estimate localized mean pixel intensity of the cells for DCF staining (more than 100 cells in each group were recorded). The fluorescence intensity in 96-well plates was quantified by Synergy™4 Multi-Mode Microplate Reader (Biotek, USA) and is normalized to mg protein in each well.

2.7. Nitric oxide generation detection

3-Amino,4-aminomethyl-2′,7′-difluorescein, diacetate (DAF-FM DA) was used as a fluorescent indicator of intracellular NO [15,16]. When HUVECs grown in petri dishes reached 80% confluence, cells were washed three times with Hanks balanced salt solution (HBSS) solution (135 mM NaCl, 5 mM KCl, 1.5 mM $CaCl_2$, 1 mM $MgCl_2$, 10 mM D-glucose, 10 mM HEPES, pH 7.40). After loading with 5 mM DAF-FM DA (Beyotime, China) at 37 °C for 20 min, the HUVECs were rinsed three times with HBSS and maintained in HBSS throughout the experiments. NO production was measured using an Olympus laser confocal scanning microscope with FITC parameter (excitation 494 nm, emission 518 nm). Images were captured randomly using constant time, exposure, and gain. The real-time recording of NO generation was also performed. As xyloketal B was added, the images were captured every 5 min for 30 min. Xyloketal B (20, 40, 60 μM) was accumulatively added to the Petri dish. For control group, endothelial nitric-oxide synthase (eNOS) inhibitor N(G)-nitro-L-arginine methyl ester (L-NAME) (100 μM, Sigma) was applied 10 min before xyloketal B treatment. Changes in $[NO]_i$ are expressed as $\Delta F/F_0$ and thus represent percent increase over basal levels.

2.8. 3-Nitrotyrosine immunofluorescence detection

HUVECs were pretreated with 0.2, 2, 20 μM xyloketal B for 30 min, respectively, followed by oxLDL (150 μg/ml) incubation for 24 h. After treatment with fresh cold 4% paraformaldehyde, cells were permeabilized with Triton X-100, and blocked for 1 h with 10% goat serum, 2% bovine serum albumin plus 0.1% Triton X-100, and then incubated with mouse monoclonal nitrotyrosine antibody (1:50, Santa Cruz Biotechnology Inc., USA) overnight at 4 °C. The cells were incubated for 30 min with Cy3-conjugated goat anti-mouse IgG (1:1000, Chemicon, USA) at room temperature. Nuclei were stained with 4',6-diamidino-2-phenylindole (DAPI, Molecular Probes, USA). The images were captured using Olympus Fluoview 500 laser confocal scanning microsopy. The mean values of Cy3-fluorescence intensity were obtained from at least three independent experiments, and at least 100 cells were quantified per Petri dish.

2.9. NADPH oxidase activity assay

Specific NADPH-dependent $O_2^{\bullet -}$ production was measured by lucigenin (5 μM) chemiluminescence as previously described [17]. The cells were pretreated with various concentration of xyloketal B or vehicle for 30 min, after which oxLDL (150 μg/ml) was added for additional 60 min. Then cells were scraped into ice-cold HBSS supplemented with 0.8 mM $MgCl_2$ and 1.8 mM $CaCl_2$, disrupted by rapid freezing in liquid nitrogen followed by sonication. Oxygen radical production was measured in the presence of 5 μM lucigenin, with or without NADPH (100 μM) for 10 min. The relative light units (RLU) of chemiluminescence were read in Turner TD 20/20 luminometer. The initial 1 min of enzyme activity was monitored. Within this time period the luminescence generation was linear. The data are expressed as RLU per second per microgram cell protein.

Table 1
PCR Primer and protocol.

Gene	PCR primer sequences	PCR protocol
gp91*phox* (687 bp)	Sense: 5′-CAACAAGAGTTCGAAGACAA-3′ Antisense: 5′-CCCCTTCTTCTTCATCTGTA-3′	95 °C/30 s 59 °C/30 s 72 °C/30 s
p47*phox* (598 bp)	Sense: 5′-AAGTGGTTTGACGGGCAG-3′ Antisense: 5′-TGGACGGAAAGTAGCCTG-3′	95 °C/30 s 60 °C/10 s 72 °C/30 s
p67*phox* (427 bp)	Sense: 5′-ATGCCTTCAGTGCCGTCCAG-3′ Antisense: 5′-TGCTTCCAGACACACTCCATCG-3′	95 °C/30 s 66 °C/30 s 72 °C/30 s
GAPDH (625 bp)	Sense: TATCGTGGAAGGACTCATGACC Antisen: TACATGGCAACTGTGAGGGG	95/30 s 55/30 s 72/1 min

2.10. RT-PCR

HUVECs were pretreated with various concentration of xyloketal B or vehicle for 30 min, after which oxLDL (150 μg/ml) was added for additional 1 h. Total RNA was extracted using Trizol (Invitrogen, USA). 1 μg of total RNA was used to perform the reverse transcription with the 2-step RT-PCR kit (Takara Bio Inc., Japan). The transcribed cDNA (1 μl) was used for polymerase chain reaction (PCR) amplification with specific primers of gp91*phox*, p47*phox*, p67*phox* and GAPDH mRNA and the PCR reaction were carried out as Table 1 [18]. GAPDH (glyceraldehydes 3-phosphate dehydrogenase) served as the loading control. The amplified products were electrophoresed on 2% agarose gels using Gel-Pro Analyzer 6.0 to analyze.

2.11. Western blot analysis for Bcl-2 protein expression

HUVECs were lysed in the RIPA lysis buffer containing protease inhibitor cocktail (Merck), The protein content of cell lysates was quantified by BCA kit, and separated by 12% SDS-PAGE and transferred onto a PVDF membrane (Millipore, USA). The membranes were blocked at room temperature for 2 h in 5% non-fat dry milk diluted with TBST (in mM: Tris–HCl 20, NaCl 150, pH 7.5, 0.1% Tween 20). The membrane was incubated overnight at 4 °C with a monoclonal rabbit anti-human Bcl-2 (1:1000 dilution; Cell Signaling Technology, USA), and then incubated for 1 h with a goat anti-rabbit IgG conjugated to horseradish peroxidase (1:10 000 dilution; Santa Cruz Biotechnology Inc. USA). The levels of Bcl-2 protein were determined using Amersham ECL™ western blotting detection reagents (GE Healthcare, UK). Incubation with polyclonal rabbit β-actin antibody (1:1000 dilution; Santa Cruz Biotechnology Inc., USA) was performed as the loading sample control. Relative density of target bands was analyzed by Gel-Pro Analyzer 6.0.

2.12. Statistics

Data are expressed as means ± S.E.M. ANOVA with post-hoc tests was used for analyzing the value between vehicle- and xyloketal B-treated group. Values of $P < 0.05$ were considered significant.

3. Results

3.1. Xyloketal B showed no toxicity in HUVECs

The new xyloketal compounds were screened for their proliferative and toxic effects on HUVECs using MTT assay. Xyloketal B at dose range between 0.3 and 160 μM alone did not exhibit either toxic or proliferative effects on HUVECs (data not shown).

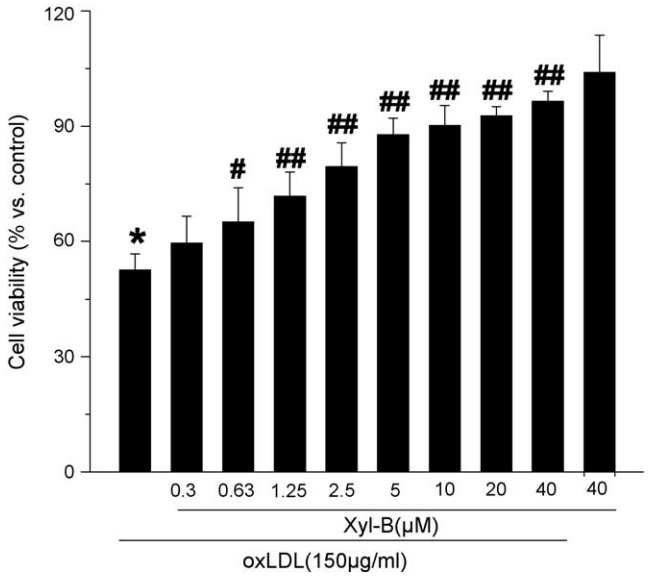

Fig. 2. Effects of xyloketal B on oxLDL-induced HUVEC injuries. Cells were grown in 96-well plates following treatment with various concentration of xyloketal B or vehicle for 30 min following treatment with oxLDL (150 gμ/ml) for 24 h. The cell viability was determined using the MTT reduction assay. Cellular viability is expressed as percentage vs. vehicle control (100%). Results are given as mean ± SEM, $n = 6$. $^{*}P < 0.01$ vs. vehicle control group, $^{\#,\#\#}P < 0.05$, 0.01 vs. HUVECs treated with oxLDL.

3.2. Xyloketal B protects endothelial cells against oxLDL-induced injury

OxLDL-induced endothelial cell injury was an early key event involved in the pathogenesis of atherosclerosis and many other cardiovascular diseases. Confluent HUVECs had a "cobblestone" mosaic appearance (Fig. 3A). Incubation with oxLDL (150 μg/ml) for 24 h induced morphological changes of HUVECs as evidenced by cell retraction and rounding up, formation of cellular fragments. In addition, oxLDL at 150 μg/ml also significantly decreased the cell viability to 52.5 ± 4% of control group ($P < 0.01$, Fig. 2). Xyloketal B significantly attenuated oxLDL-induced both morphological changes and decrease in cellular viability in a concentration-dependent manner and the IC_{50} value was 1.5 μM.

3.3. Xyloketal B inhibits oxLDL-induced HUVEC apoptosis and Bcl-2 expression

To examine whether xyloketal B can inhibit oxLDL-induced HUVEC apoptosis, DAPI staining was performed to examine late stage morphological indicators of apoptosis such as nuclear segmentation and chromatin condensation. Incubation with 150 μg/ml oxLDL for 24 h significantly induced cell shrinkage, nuclear segmentation, and chromatin condensation (highlighted by arrows, Fig. 3B). Compared with HUVECs, 150 μg/ml oxLDL increased the percentage of apoptotic cells from 3.8 ± 1% to 24.7 ± 1.3%. Preincubation with xyloketal B at 0.2, 2 and 20 μM significantly reduced the percentage of oxLDL-induced apoptotic HUVECs from 24.7 ± 1.3% to 23.4 ± 3.9%, 11.9 ± 1.9%, and 8.0 ± 1.4%, respectively ($P < 0.05$, Fig. 3C).

Stimulation with oxLDL at 150 μg/ml for 24 h significantly decreased the Bcl-2 protein expression to 61 ± 14% of control HUVECs, whereas xyloketal B at 2 and 20 μM attenuated oxLDL-induced downregulation of Bcl-2 expression (90.6 ± 4.0% and 107 ± 9.5% of control HUVECs, respectively, $P < 0.05$, Fig. 3D and E).

3.4. Xyloketal B inhibits ROS production induced by oxLDL in HUVECs

As shown in Fig. 4A, pretreatment with xyloketal B significantly reduced oxLDL-stimulated DCF fluorescence intensity in a concentration-dependent manner. Xyloketal B at 1 and 40 μM significantly inhibited oxLDL-induced ROS production by 22% and 67% ($P < 0.05$, Fig. 4B).

3.5. Xyloketal B reduces oxLDL-stimulated NADPH oxidase activity

As shown in Fig. 5A, oxLDL-induced $O_2^{\bullet -}$ production in endothelial cells was dependent on the presence of NADPH (100 μM). Incubation of HUVECs with oxLDL (150 μg/ml) for 1 h increased the NADPH oxidase activity by 128% ($P < 0.01$). Xyloketal B significantly attenuated oxLDL-stimulated NADPH oxidase activity. Xyloketal B at 2 and 20 μM significantly reduced NADPH oxidase activity of HUVECs from 76.3 ± 2.6 RLU/s/mg protein to 55.6 ± 6.2 RLU/s/mg protein and 45.6 ± 5.5 RLU/s/mg protein, respectively ($P < 0.01$, Fig. 5B). NADPH oxidase inhibitor, apocynin at 10 μM completely abolished oxLDL-stimulated NADPH oxidase activity ($P < 0.01$, Fig. 5A).

3.6. Xyloketal B inhibits overexpression of gp91phox and p47phox mRNA

As shown in Fig. 5C and D, gp91*phox*, p47*phox* and p67*phox* mRNA expression significantly increased in response to oxLDL in HUVECs, [18]. Xyloketal B at 20 μM significantly inhibited oxLDL-induced mRNA expression of gp91*phox* (107 ± 11 vs. 165 ± 11, $P < 0.05$, $n = 3$) and p47*phox* (135 ± 7 vs. 175 ± 13, $P < 0.05$, $n = 3$) but not p67*phox* (151 ± 9 vs. 154 ± 8, $P > 0.05$, $n = 3$).

3.7. Effects of xyloketal B on oxLDL-stimulated endothelial $ONOO^-$ levels

Excessive ROS in endothelial cells easily reacts with NO to form peroxynitrite ($ONOO^-$). We investigated whether xyloketal B can inhibit $ONOO^-$ production using 3-nitrotyrosine (3-NT) as the indicator of $ONOO^-$ production [19]. As shown in Fig. 6A and B, 150 μg/ml oxLDL for 24 h significantly increased the 3-NT level in HUVECs, however, xyloketal B at 2 and 20 μM as well as apocynin (10 μM) attenuated oxLDL-induced augmentation of the 3-NT level.

3.8. Xyloketal B promotes NO release of endothelial cells

We further investigated whether xyloketal B affects endothelial NO generation. As reported in Fig. 7A–D, xyloketal B time- and concentration-dependently enhanced NO release in HUVECs. The xyloketal B induced NO release was completely inhibited by eNOS inhibitor, L-NAME (100 μM).

4. Discussion

In this study, we investigated the protective effects of xyloketal B in a model of oxidized LDL-induced endothelial cell injury. To our knowledge, we have demonstrated for the first time that xyloketal B significantly reduces oxLDL-induced endothelial cell injury in a dose dependent manner. In parallel with its protective action, xyloketal B suppresses ROS production, peroxynitrite formation and promotes NO production in HUVECs. Furthermore, xyloketal B significantly inhibits NADPH oxidase activity as well as the mRNA expression of gp91*phox* and p47*phox*, suggesting that NADPH oxidase, especially gp91 containing *phox* and p47 containing *phox* may be a potential action target of xyloketal B. Xyloketal B appears to be quite safe because xyloketal B at 160 μM does not cause toxic or proliferative effects on endothelial cells.

The oxLDL-mediated injury to endothelial cells is crucial for endothelial dysfunction in early atherosclerosis and atherosclerotic plaque rupture in the advanced stage [20]. Therefore, the in

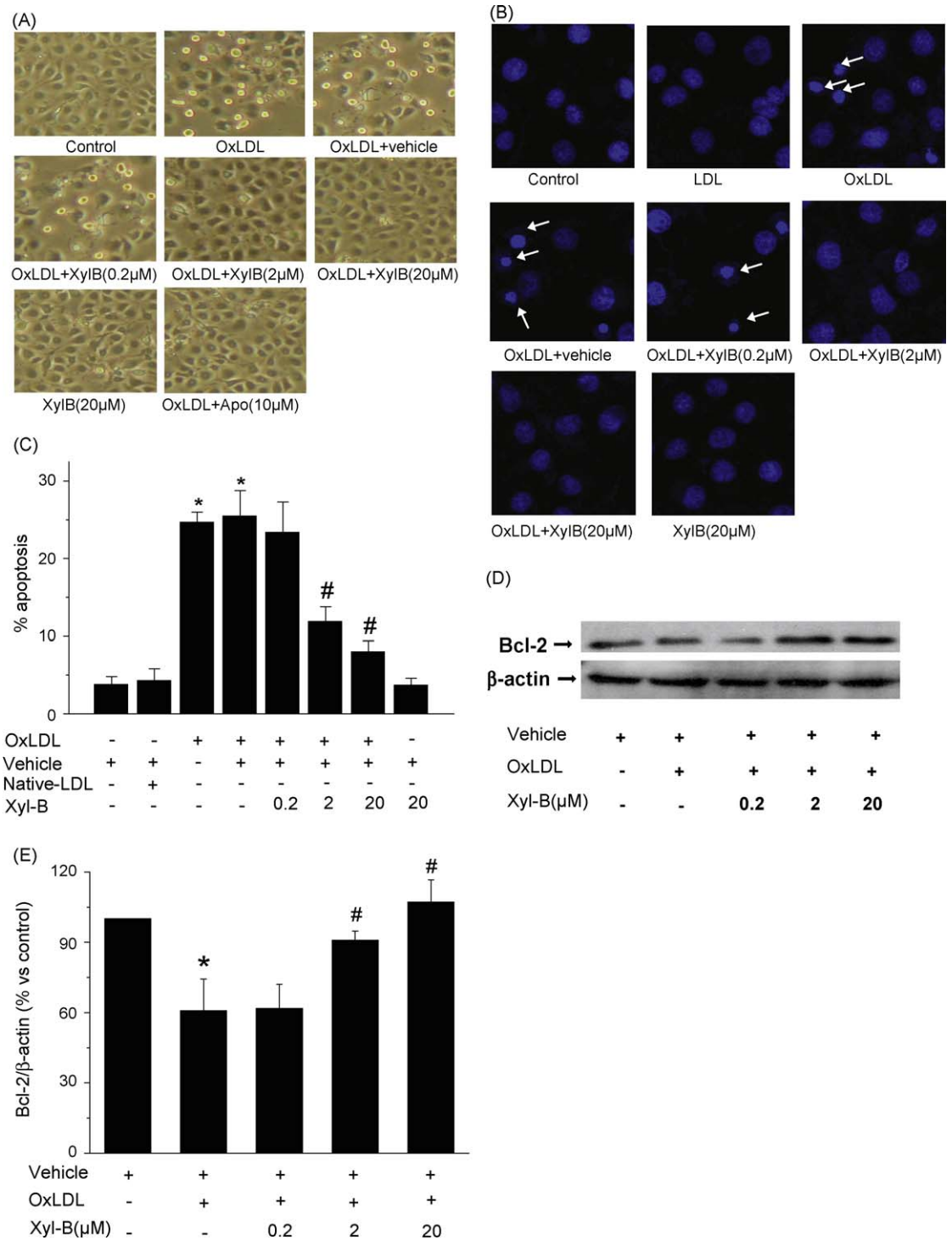

Fig. 3. Effects of xyloketal B on oxLDL-induced endothelial injury. Cells were preincubated with xyloketal B for 30 min, and then exposed to 150 μg/ml oxLDL for further 24 h. (A) Cellular morphological changes were detected by inverted microscopy. Cells pretreated with 10 μM apocynin (Apo) were taken as positive control. (B) DAPI staining was employed to detect apoptotic cell death. Representative images were selected from six independent experiments. Cellular pyknosis is indicated with white arrow. (C) the mean values of percentages of apoptotic cells were summarized after DAPI staining, $^{*}P < 0.01$ vs. vehicle control, $^{\#}P < 0.01$ vs. HUVECs treated with oxLDL, $n = 6$. (D) Western blot analysis of Bcl-2 expression in cells representative images was selected from three independent experiments. (E) The mean value of Bcl-2 expression in each treatment group was normalized to the vehicle control group. $^{*}P < 0.05$ vs. vehicle control, $^{\#}P < 0.05$ vs. HUVECs treated with oxLDL, $n = 3$.

vitro model of oxLDL-induced endothelial cell injury has been applied to mimic the oxidative endothelial injury during atherogenesis [21,22]. Consistent with previous reports, we found that oxLDL-induced significant endothelial cell injury and decreased Bcl-2 protein expression [22]. In contrast, xyloketal B treatment dramatically reduced oxLDL-induced endothelial cell injury and attenuated oxLDL-induced Bcl-2 protein expression. It is reported that Bcl-2 is an anti-apoptotic protein that can inhibit apoptosis induced by a mitochondria-dependent caspase-9 pathway [23]. Bcl-2 has also been shown to prevent apoptosis induced by diverse stimuli by inhibiting the mitochondrial release of cytochrome c that stimulates caspase-9 activity or by

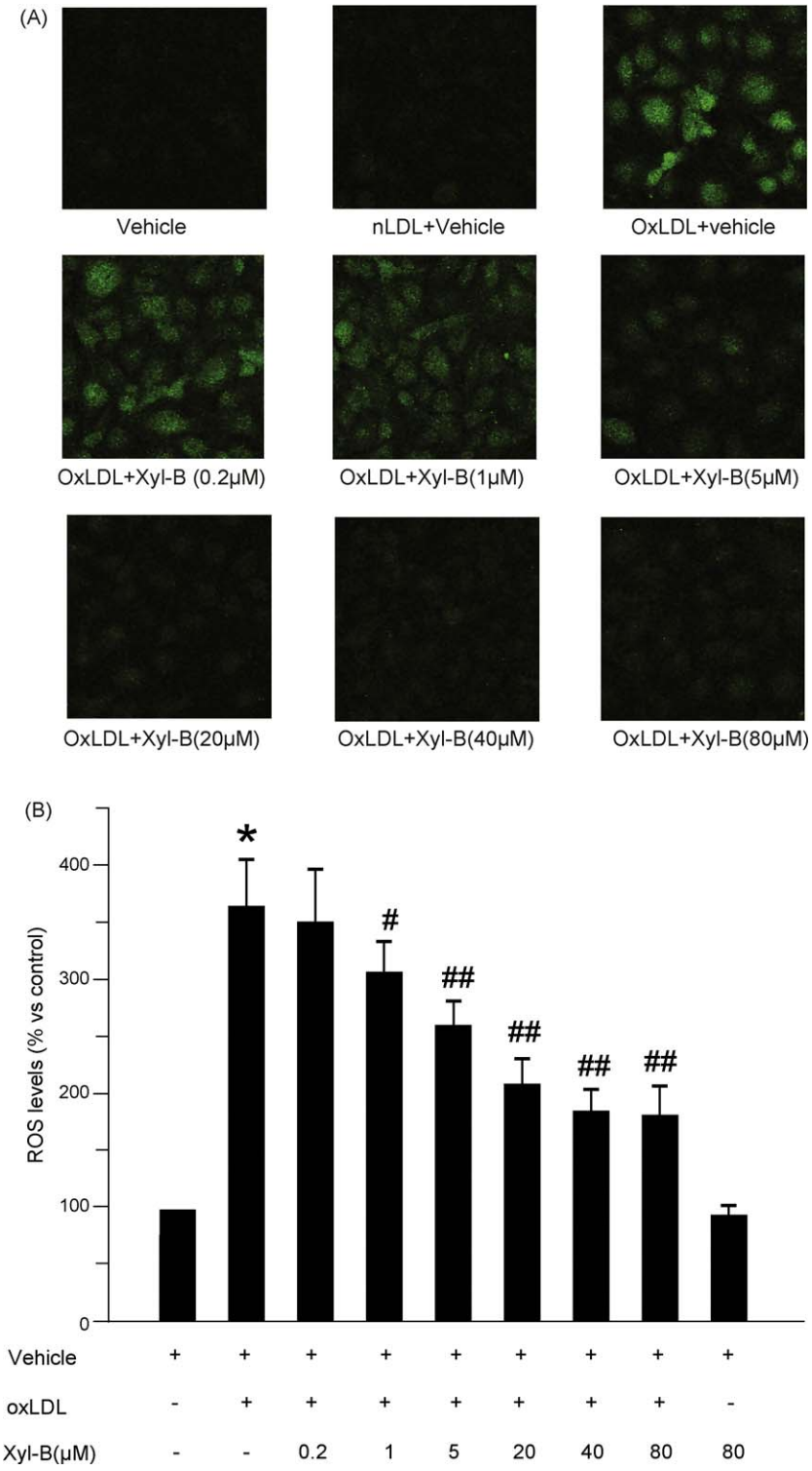

Fig. 4. Effects of xyloketal B on oxLDL-stimulated endothelial ROS production. (A) HUVECs were seeded in Petri dish. After 1 h incubation with DCFH-DA (10 μM), cells were pretreated with xyloketal B for 30 min, and further incubated with oxLDL (150 μg/ml) for additional 60 min. The representative images were from three independent experiments (200×). (B) Cells were seeded in clear bottom black 96 wells plates. Then cells were treated as above description. The DCFH-DA fluorescence intensity was measured in Multi-Mode Microplate Reader. ('*' vs. control, $P < 0.01$, '#, ##' vs. oxLDL group, $P < 0.05$ and 0.01, respectively, $n = 6$).

acting as an antioxidant [24]. Overexpression of the Bcl-2 gene inhibits apoptosis in murine aortic endothelial cells [25]. Therefore, the protective action of xyloketal B on oxLDL-induced endothelial cell injury is probably related to restoration of Bcl-2 protein expression. In addition, since the intrinsic apoptotic pathway hinges on the balance between pro- and anti-apoptotic members of the Bcl-2 family, such as Bax, Bcl-X(L), Bak and Bad [26–28], the effects of xyloketal B on the pro-apoptotic proteins need further study.

OxLDL-induced apoptosis mainly through oxidative stress. Consistent with literature, we found that generation of ROS in particular of $O_2^{\bullet-}$ and proxynitrite was induced in HUVECs in

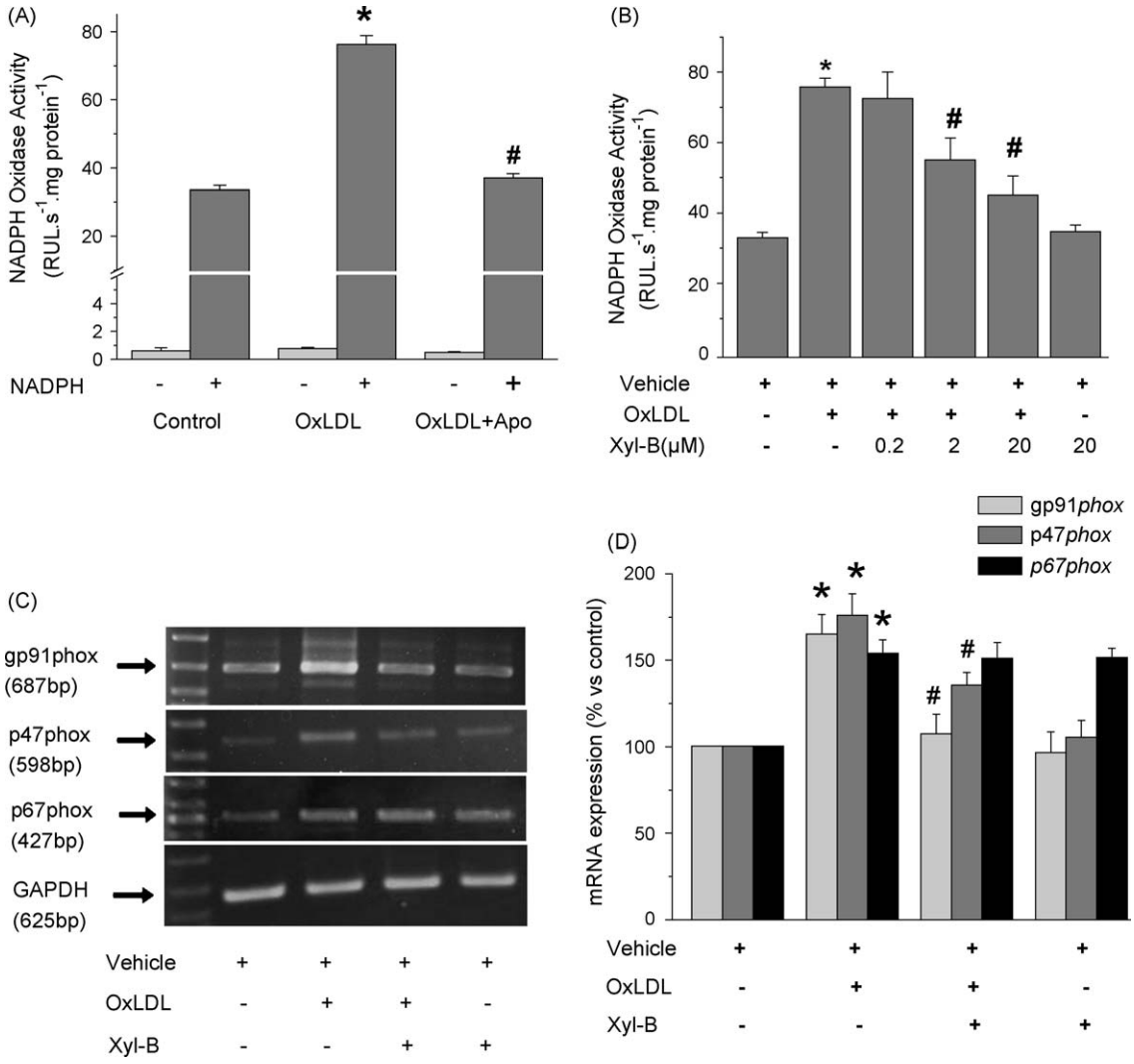

Fig. 5. Effects of xyloketal B on NADPH oxidase activity. Cells were preincubated with xyloketal B for 30 min and further incubated with oxLDL (150 μg/ml) for additional 60 min. (A) and (B) Oxygen radical production was measured in the presence of 5 μM lucigenin, with or without NADPH (100 μM) for 10 min. The reaction was started by the addition of NADPH (100 μM), and the relative light units (RLU) of chemiluminescence were read in Turner TD 20/20 luminometer. ('*' vs. vehicle control, '#' vs. ox-LDL group, $P < 0.01$, $n = 4$). (C) and (D) OxLDL led to increase in gp91*phox*, p47*phox*, and p67*phox* mRNA expression. Xyloketal B (20 μM) attenuated oxLDL-induced increase in gp91*phox* and p47*phox* mRNA expression but not p67*phox* mRNA overexpression. ('*' vs. control, '#' vs. oxLDL treated group, $P < 0.05$, $n = 3$).

response to oxLDL. The overproduction of ROS and proxynitrite was significantly inhibited by xyloketal B. NADPH oxidase is recognized as the major source of ROS in vascular cells, including endothelial cells and the increased NADPH activity has been detected in atherosclerotic arteries [29]. All the components of the phagocyte NADPH oxidase complex, including two membrane-bound proteins, gp91*phox* and p22*phox*, and two cytosolic proteins, p47*phox* and p67*phox*, have been identified in endothelial cell [30]. Nonphagocytic NADPH oxidase is constitutively active, and its activity is sensitively affected by a wide variety of pathophysiological stimuli [31]. A rapid post-translational activation and/or an increased expression of oxidase subunits can be involved in the upregulation of NADPH oxidase activity [32]. For example, endothelial NADPH oxidase activity is increased by angiotensin II [33], ischemia [34], and oxLDL [18]. OxLDL has been shown to induce proatherosclerotic NADPH oxidase expression by increasing gp91*phox* mRNA expression [18]. We here found that the activity of NADPH and mRNA expression of gp91*phox* and p47*phox* in HUVECs were increased in response to oxLDL stimulation. Xyloketal B significantly reduced oxLDL-induced activity of NADPH and mRNA expression of gp91*phox* and p47*phox*. In addition, xyloketal B treatment significantly reduced the mRNA expression of gp91*phox* and p47*phox*, but not p67*phox*, indicating this compound possibly has selectively inhibitory effects on NADPH oxidase subunits.

The disturbed balance between NO and reactive oxygen species (ROS) plays an important role in vascular abnormality during atherosclerosis and other cardiovascular diseases. Decreased NO levels are coupled with impaired endothelium-dependent vasodilation during many cardiovascular diseases. Increasing endothelial-dependent NO release is believed to benefit to cardiovascular system. For example, several calcium channel blockers (CCBs) and HMG-CoA reductase inhibitors (statins) have been shown to improve endothelial-dependent NO release and thereby preventing plaque progression in atherosclerosis [35]. In the present study, xyloketal B stimulated NO production in HUVECs in a time- and concentration-dependent manner. The NO production induced by xyloketal B may be derived from eNOS because xyloketal B induced NO production can be completely abolished by L-NAME, an eNOS inhibitor. Nevertheless, given that both intracellular and extracellular NO donors have been confirmed to inhibit oxLDL-induced

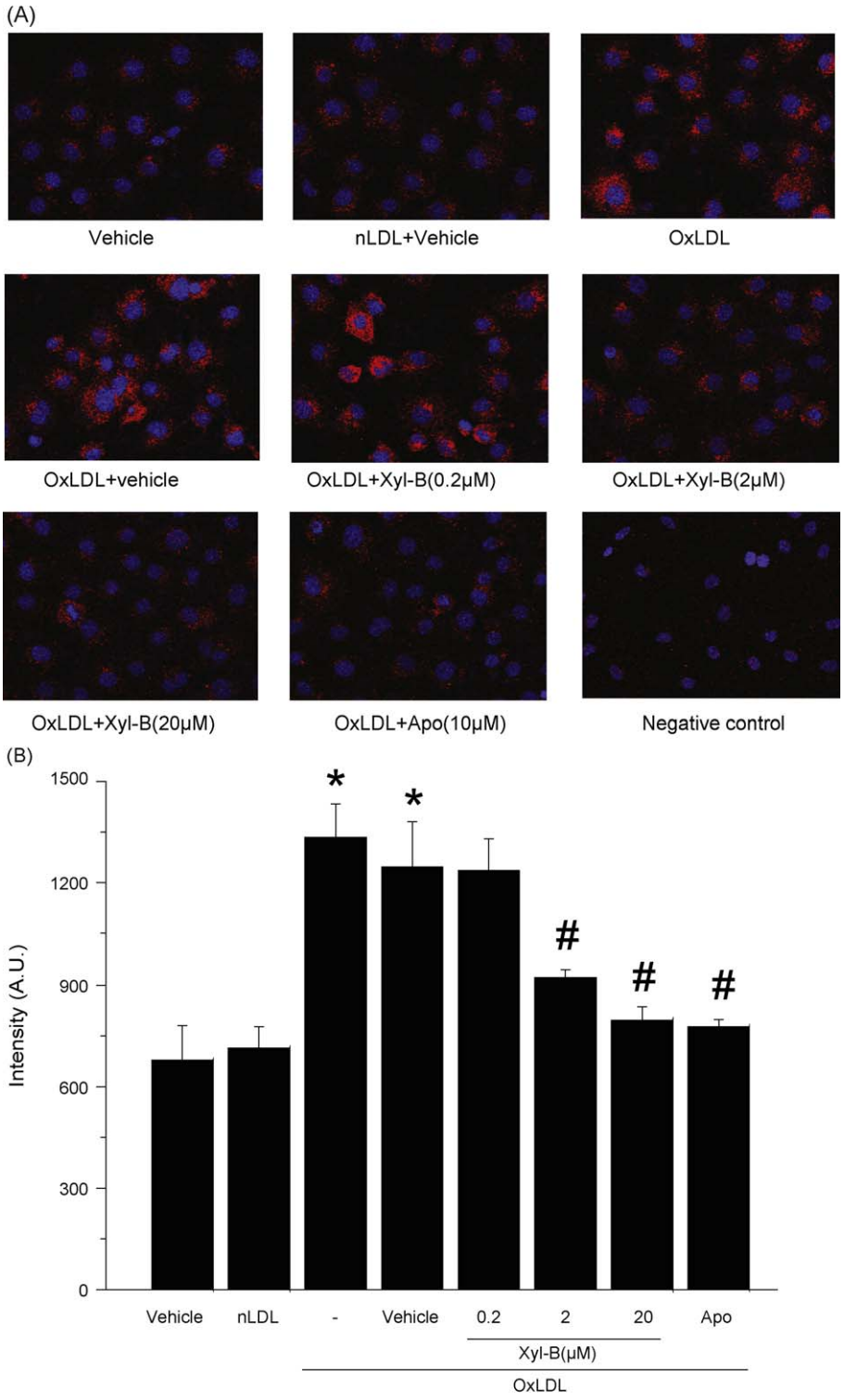

Fig. 6. Effects of xyloketal B on oxLDL-stimulated endothelial $ONOO^-$ levels. 3-nitrotyrosine (3-NT) is the maker of $ONOO^-$. (A) OxLDL (150 μg/ml) but not native LDL (150 μg/ml) increased 3-NT expression. Pretreatment with xyloketal B at 2 and 20 μM but not 0.2 μM for 30 min inhibited oxLDL-induced 3-NT expression in HUVECs. Apocynin (10 μM) also inhibited oxLDL-induced 3-NT expression in HUVECs. (B) Analysis of fluorescence of 3-NT expression in HUVECs. ('*' vs. control, '#' vs. oxLDL treatment group, $P < 0.01$, $n = 3$).

apoptotic endothelial cell death through scavenging cellular lipid peroxyl radicals and restoring the Bcl-2 protein expression [36,37], the augmentation of NO production may be at least one of protective mechanisms of xyloketal B.

In summary, the present study reveals that xyloketal B protects HUVECs from oxLDL-induced injury probably through multiple mechanisms mainly involved attenuation of oxLDL-induced oxidative stress, and enhancement of endothelial NO release, making it a promising compound for further evaluation in the treatment of atherosclerosis. Further studies addressing the effects of xyloketal B in cardiovascular disease models will provide much evidence for better understanding the pharmacological profile of xyloketal B.

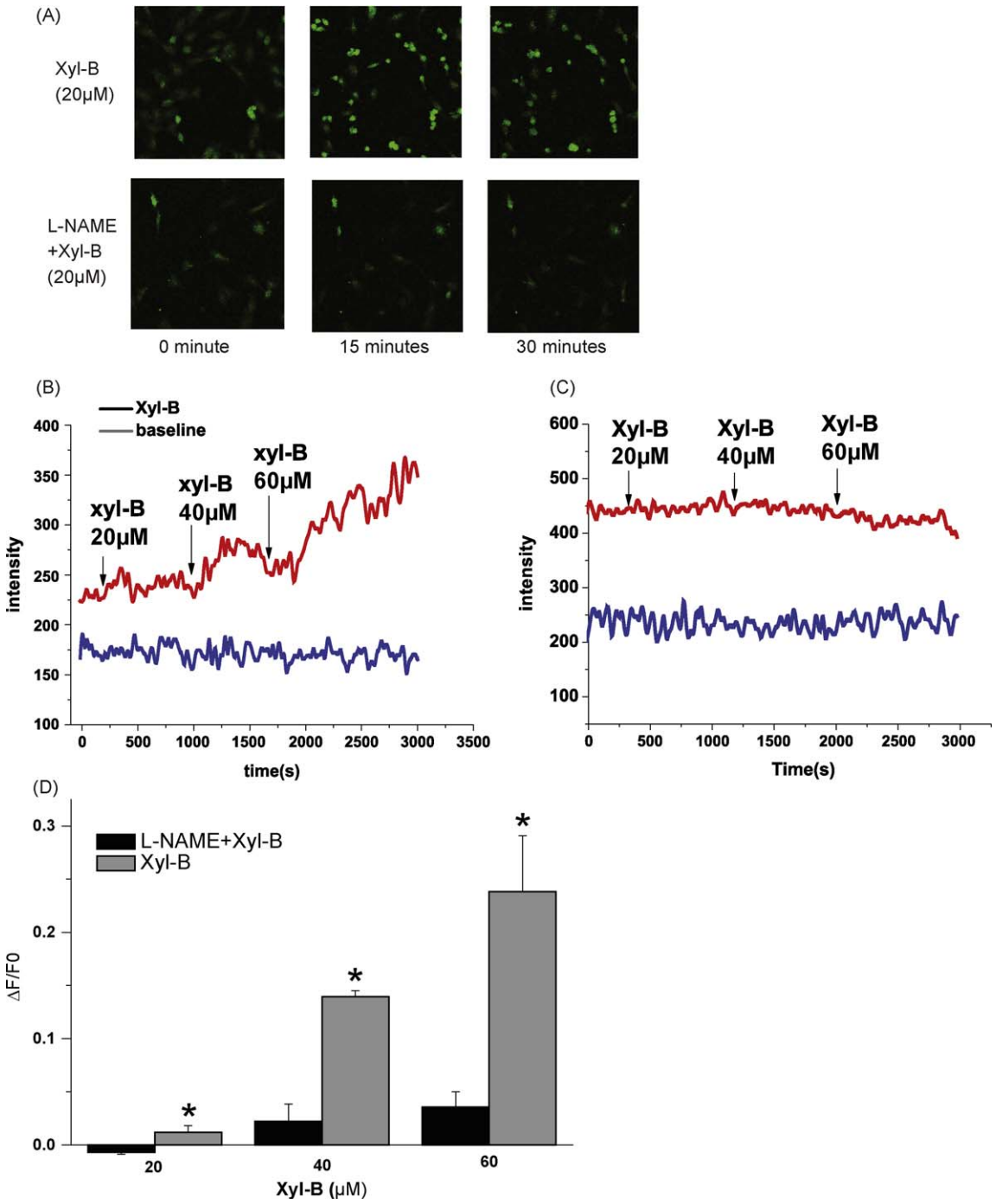

Fig. 7. Effects of xyloketal B on NO release in HUVECs. (A), after incubation with DAF-FM DA, cells were treated with 20 μM xyloketal B. The fluorescence intensity changes were monitored by confocal scanning microscope. Images were taken with the interval of 5 min. Xyloketal B can enhance endothelial NO release time-dependently which could be completely reversed by eNOS inhibitor, L-NAME (100 μM) Representative images were from three independent experiments ('*' vs. L-NAME group, $P < 0.01$, $n = 3$). (B–D), the effect of xyloketal B on NO release was measured using real-time confocal recording.

Acknowledgments

This work was supported by the 863 project (2006AA09Z440) from the Ministry of Science, Technology of the People's Republic of China and by National Natural Science Foundation of China (no. 30873059), the Scientific Research Foundation for the Returned Overseas Chinese Scholars, State Education Ministry (2007,1108#) and Team Project of Nature Science Foundation of Guangdong Province, China, grant 06201946.

Appendix A. Supplementary data

Supplementary data associated with this article can be found, in the online version, at doi:10.1016/j.bcp.2009.05.029.

References

[1] Ross R. Atherosclerosis is an inflammatory disease. Am Heart J 1999;138: S419–20.

[2] Sawamura T, Kume N, Aoyama T, Moriwaki H, Hoshikawa H, Aiba Y, et al. An endothelial receptor for oxidized low-density lipoprotein. Nature 1997;386:73–7.
[3] Cominacini L, Pasini AF, Garbin U, Davoli A, Tosetti ML, Campagnola M, et al. Oxidized low density lipoprotein (ox-LDL) binding to ox-LDL receptor-1 in endothelial cells induces the activation of NF-kappaB through an increased production of intracellular reactive oxygen species. J Biol Chem 2000;275:12633–8.
[4] Radomski MW, Palmer RM, Moncada S. Comparative pharmacology of endothelium-derived relaxing factor, nitric oxide and prostacyclin in platelets. Br Journal Pharmacol 1987;92:181–7.
[5] Viappiani S, Schulz R. Detection of specific nitrotyrosine-modified proteins as a marker of oxidative stress in cardiovascular disease. Am J Physiol Heart Circ Physiol 2006;290:H2167–8.
[6] Reiter CD, Teng RJ, Beckman JS. Superoxide reacts with nitric oxide to nitrate tyrosine at physiological pH via peroxynitrite. J Biol Chem 2000;275:32460–6.
[7] Davignon J, Ganz P. Role of endothelial dysfunction in atherosclerosis. Circulation 2004;109:III27–32.
[8] Mayer AM, Gustafson KR. Marine pharmacology in 2000: antitumor and cytotoxic compounds. Int J Cancer 2003;105:291–9.
[9] Lin Y, Wu X, Feng S, Jiang G, Luo J, Zhou S, et al. Five unique compounds: xyloketals from mangrove fungus *Xylaria* sp. from the South China sea coast. J Org Chem 2001;66:6252–6.
[10] Pettigrew JD, Wilson PD. Synthesis of xyloketal A, B, C, D, and G analogues. J Org Chem 2006;71:1620–5.
[11] Jaffe EA, Nachman RL, Becker CG, Minick CR. Culture of human endothelial cells derived from umbilical veins. Identification by morphologic and immunologic criteria. J Clin Invest 1973;52:2745–56.
[12] Redgrave TG, Roberts DC, West CE. Separation of plasma lipoproteins by density-gradient ultracentrifugation. Anal Biochem 1975;65:42–9.
[13] Steinbrecher UP, Witztum JL, Parthasarathy S, Steinberg D. Decrease in reactive amino groups during oxidation or endothelial cell modification of LDL. Correlation with changes in receptor-mediated catabolism. Arteriosclerosis (Dallas TX) 1987;7:135–43.
[14] Royall JA, Ischiropoulos H. Evaluation of 2′,7′-dichlorofluorescin and dihydrorhodamine 123 as fluorescent probes for intracellular H_2O_2 in cultured endothelial cells. Arch Biochem Biophys 1993;302:348–55.
[15] Kojima H, Urano Y, Kikuchi K, Higuchi T, Hirata Y, Nagano T. Fluorescent indicators for imaging nitric oxide production. Angew Chem Int Ed Engl 1999;38:3209–12.
[16] Zheng X, Ning G, Hong D, Zhang M. Nitric oxide imaging in neurons using confocal microscopy. Methods Mol Biol 2004;279:69–80.
[17] Vaquero EC, Edderkaoui M, Pandol SJ, Gukovsky I, Gukovskaya AS. Reactive oxygen species produced by NAD(P)H oxidase inhibit apoptosis in pancreatic cancer cells. J Boil Chem 2004;279:34643–54.
[18] Rueckschloss U, Galle J, Holtz J, Zerkowski HR, Morawietz H. Induction of NAD(P)H oxidase by oxidized low-density lipoprotein in human endothelial cells: antioxidative potential of hydroxymethylglutaryl coenzyme A reductase inhibitor therapy. Circulation 2001;104:1767–72.
[19] Sucu N, Unlu A, Tamer L, Aytacoglu B, Ercan B, Dikmengil M, et al. 3-Nitrotyrosine in atherosclerotic blood vessels. Clin Chem Lab Med 2003;41:23–5.
[20] Li D, Mehta JL. Antisense to LOX-1 inhibits oxidized LDL-mediated upregulation of monocyte chemoattractant protein-1 and monocyte adhesion to human coronary artery endothelial cells. Circulation 2000;101:2889–95.
[21] Kume N, Kita T. Apoptosis of vascular cells by oxidized LDL: involvement of caspases and LOX-1 and its implication in atherosclerotic plaque rupture. Circ Res 2004;94:269–70.
[22] Chen J, Mehta JL, Haider N, Zhang X, Narula J, Li D. Role of caspases in Ox-LDL-induced apoptotic cascade in human coronary artery endothelial cells. Circ Res 2004;94:370–6.
[23] Kane DJ, Sarafian TA, Anton R, Hahn H, Gralla EB, Valentine JS, et al. Bcl-2 inhibition of neural death: decreased generation of reactive oxygen species. Science 1993;262:1274–7.
[24] Hockenbery DM, Oltvai ZN, Yin XM, Milliman CL, Korsmeyer SJ. Bcl-2 functions in an antioxidant pathway to prevent apoptosis. Cell 1993;75:241–51.
[25] Kondo S, Yin D, Aoki T, Takahashi JA, Morimura T. Takeuchi J. bcl-2 gene prevents apoptosis of basic fibroblast growth factor-deprived murine aortic endothelial cells. Exp Cell Res 1994;213:428–32.
[26] Shroff EH, Snyder C, Chandel NS. Role of Bcl-2 family members in anoxia induced cell death. Cell Cycle 2007;6:807–9.
[27] Wong WW, Puthalakath H. Bcl-2 family proteins: the sentinels of the mitochondrial apoptosis pathway. IUBMB Life 2008;60:390–7.
[28] Lalier L, Cartron PF, Juin P, Nedelkina S, Manon S, Bechinger B, et al. Bax activation and mitochondrial insertion during apoptosis. Apoptosis 2007;12:887–96.
[29] Lassegue B, Clempus RE. Vascular NAD(P)H oxidases: specific features, expression, and regulation. Am J Physiol Regul Integr Comp Physiol 2003;285:R277–97.
[30] Mohazzab KM, Kaminski PM, Wolin MS. NADH oxidoreductase is a major source of superoxide anion in bovine coronary artery endothelium. Am J Physiol 1994;266:H2568–72.
[31] Cai H, Harrison DG. Endothelial dysfunction in cardiovascular diseases: the role of oxidant stress. Circ Res 2000;87:840–4.
[32] Gorlach A, Brandes RP, Nguyen K, Amidi M, Dehghani F, Busse R. A gp91phox containing NADPH oxidase selectively expressed in endothelial cells is a major source of oxygen radical generation in the arterial wall. Circ Res 2000;87:26–32.
[33] Li JM, Shah AM. Mechanism of endothelial cell NADPH oxidase activation by angiotensin II. Role of the p47phox subunit. J Biol Chem 2003;278:12094–100.
[34] Tojo T, Ushio-Fukai M, Yamaoka-Tojo M, Ikeda S, Patrushev N, Alexander RW. Role of gp91phox (Nox2)-containing NAD(P)H oxidase in angiogenesis in response to hindlimb ischemia. Circulation 2005;111:2347–55.
[35] Delsing DJ, Jukema JW, van de Wiel MA, Emeis JJ, van der Laarse A, Havekes LM, et al. Differential effects of amlodipine and atorvastatin treatment and their combination on atherosclerosis in ApoE*3-Leiden transgenic mice. J Cardiovasc Pharmacol 2003;42:63–70.
[36] Kotamraju S, Hogg N, Joseph J, Keefer LK, Kalyanaraman B. Inhibition of oxidized low-density lipoprotein-induced apoptosis in endothelial cells by nitric oxide. Peroxyl radical scavenging as an antiapoptotic mechanism. J Biol Chem 2001;276:17316–23.
[37] Hacker A, Muller S, Meyer W, Kojda G. The nitric oxide donor pentaerythritol tetranitrate can preserve endothelial function in established atherosclerosis. Br J Pharmacol 2001;132:1707–14.